**M. Mohandes**
Professor
Department of Electrical Engineering
King Fahd University of Petroleum &
Minerals, Dhahran-31261
Saudi Arabia

**S. Rehman**
Research Engineer
Interdisplinary Research Center for
Renewable Energy and Power Systems
Research Institute
King Fahd University of Petroleum &
Minerals, Dhahran-31261
Saudi Arabia

**H. Nuha**
Assistant Professor
HUMIC, School of Computing
Telkom University
Indonesia

**M.S. Islam**
Student
Department of Electrical Engineering
King Fahd University of Petroleum &
Minerals, Dhahran-31261, Saudi Arabia

**F.H. Schulze**
Managing Director
CESI Middle East
UAE

# Accuracy of Wind Speed Predictability with Heights using Recurrent Neural Networks

*Accurate prediction of wind speed in future time domain is critical for wind power integration into the grid. Wind speed is usually measured at lower heights while the hub heights of modern wind turbines are much higher in the range of 80-120m. This study attempts to better understand the predictability of wind speed with height. To achieve this, wind data was collected using Laser Illuminated Detection and Ranging (LiDAR) system at 20m, 40m, 50m, 60m, 80m, 100m, 120m, 140m, 160m, and 180m heights. This hourly averaged data is used for training and testing a Recurrent Neural Network (RNN) for the prediction of wind speed for each of the future 12 hours, using 48 previous values. Detailed analyses of short-term wind speed prediction at different heights and future hours show that wind speed is predicted more accurately at higher heights.For example, the mean absolute percent error decreases from 0.19 to 0.16as the height increase from 20m to 180m, respectively for the 12$^{th}$ future hour prediction. The performance of the proposed method is compared with Multilayer Perceptron (MLP) method. Results show that RNN performed better than MLP for most of the cases presented here at the future 6th hour.*

***Keywords:****Short Term Forecasting; Wind Speed Prediction with heights; Recurrent Neural Network; Multilayer perceptron.*

## 1. INTRODUCTION

Exponentially growing population and at the same or even at higher pace increasing power demands are the concerns of people from all walks of life. Renewable energy penetration into the energy mix and wind in particular is increasing globally due to its environ–mentallyfriendly nature, fast technological development, commercial acceptance, ease of operation and main–tenance, and competitive cost. Additionally, the deploy–ment of wind power projects reduces the dependence on fossil fuels and consequently cut down the greenhouse gases (GHG) emissions into the local atmosphere. As a sign of progress in wind power sector, in 2020, the cumulative global wind power installed capacity reached 743 GW with new addition of 93 GW [1,2]. At present, there are more than 90 countries cont–ributing towards wind power capacity build up inc–luding 9 countries with more than 10 GW and 29 more than 1 GW of installed capacities globally.

Wind speed, among all the meteorological para–me–ters, is highly fluctuating both in temporal and spatial domains. It changes with time of the day, month of the year, and day of the year. This fluctuating nature of wind speed creates an uncertainty in the availability of continuous power and more importantly the stability of the grid. Hence, understanding the variability of the wind speed at a location with time is critical for quality and magnitude of wind energy yield, which is directly proportional to the cube of wind speed. It simply means that proper understanding of the wind speed variations based on long-term historical wind data and its future trends is a pre-requisite for the success of huge investments. Hence, when planning the deployment of a farm at a site, an indispensable task is to conduct on-site wind speed measurements at least for one complete year (the longer the better) and analyse it to extract information on the variability of the wind [3–12]. The variability of wind covers a wide spectrum of time-scales starting from seconds, hours, days, months, year, and to several years. So, predicting the wind speed accurately ahead of time, few hours to days, is important for power producers, grid operators, energy managers, and lastly the consumers [13–15]. Advanced but accurate knowledge of wind speed availability ahead of time can be utilized in applications, such as wind power dispatch planning, power quality, grid operation, reserve allocation, and generation scheduling.

Artificial intelligence techniques such as Artificial Neural Networks (ANN)[9], Convolution LSTM Net–works [16], neuro-fuzzy systems [17], support vector machines [18], long-short term memory networks [19], Particle Swarm Optimization (PSO) [20],modes decom–position based low rank multi-kernel ridge regre–ssion [21], Gaussian process regression combined with nume–rical weather predictions [22], Singular Spectrum Analysis and Adaptive Neuro Fuzzy Inference System [23], optimal feature selection and a modified bat algorithm with the cognition strategy [24], and spatial model[25] have been applied to capture the nonlinear

Received: March 2021, Accepted: August 2021
Correspondence to: Dr. Shafiqur Rehman, Research Institute, King Fahd University of Petroleum & Minerals, Dhahran-31261, Saudi Arabia
E-mail: srehman@kfupm.edu.sa
**doi:10.5937/fme2104908M**

trend of the wind speed data series. Since early 2000, the trend of using hybrid methodologies has emerged in the literature in which more than one models is combined to achieve better forecasts of wind speed in future and spatial domains [26–28]. These modern machine learning methods are very useful and provide relatively better estimates both in time and spatial domains as can be seen from wide ranging applications like perfor–mance prediction of thermosiphon solar water heaters [29], analysis of absorption systems [30], sizing of pho–tovoltaic systems [31,32] ground conductivity map generation [33], and solar radiation forecasting [34].

Akçay and Filik[35] developed a framework based on data de-trending, covariance-factorization via sub–space method and one and/or multi-step-ahead Kalman filter for the prediction of wind speed. The numerical experiments on the real data sets showed that the wind speed forecast particularly using multi-step-ahead filter outperformed persistence model-based predictions. In another study, Filik and Filik [36]used ANN based models in conjunction with weather parameters like ambient temperature and pressure and found good agreement between the measured and predicted values of wind speed. Santamaría-Bonfil et al. [37] predicted wind speeds 1-24 hours ahead using hybrid metho–do–logy comprised of Support Vector Regression and sho–wed better forecast compared to persistence and autoregressive models. Hu et al. [38] introduced deep learning neural network technique to predict the wind speed and showed that the proposed approach reduced significantly the error between the predicted and measured values.

Kang et al. [39]proposed a hybrid Ensemble Empi–rical Mode Decomposition (EEMD) and Least Square Support Vector Machine (LSSVM) model to improve short-term wind speed forecasting precision. The results showed that the proposed hybrid model outperformed some of the existing methods such as Back Propagation Neural Networks (BP), Auto-Regressive Integrated Mo–ving Average (ARIMA), and combination of Empirical Mode Decomposition (EMD). Liu et al. [40] used combination of Secondary Decomposition Algorithm (SDA) and the Elman neural networks and showed that the hybrid model performed better than the multi-step wind speed predictions. Wang et al.[41]showed that Least Square Support Vector Machine and the Markov hybrid model performed better than other models for wind speed prediction. Marović et al. [42] proposed ANN based wind speed prediction model for imp–lementation in the early warning system to announce the possibility of the harmful phenomena occurrence due to winds, which proved to be accurate in terms of alerting the community ahead of time due to bad wind con–ditions. Shukur and Lee [43]used artificial neural net–work and Kalman filter hybrid model to address the nonlinearity and uncertainty issues and reported to be accurate in comparison with measured values. Jianzhou et al.[44], used support vector regression combined with seasonal index adjustment and Elman recurrent neural network techniques and obtained relatively better forecast compared to other models.

Koo et al. [45]evaluated the accuracy of the wind-speed prediction using artificial neural networks in terms of correlation coefficients between actual and simulated wind-speed data for plain, coastal, and mountainous areas. The study concluded that the geog–raphical location played important role in prediction accuracy of wind speed. For hourly prediction, Wu et al. [46] integrated single multiplicative neuron model with iterated nonlinear filters for updating the wind speed sequence accurately. The results indicated better per–formance of the proposed model compared to autoreg–ressive moving average, artificial neural network, kernel ridge regression based residual active learning and single multiplicative neuron models. Zhang et al. [47] used hybrid models (combination of empirical mode decomposition, feature selection with artificial neural network, and support vector machine) for short term wind speed prediction and found better results compared to single ANN, SVM, traditional EMD-based ANN and EMD-based SVM models. Doucoure et al. [48] used multi-resolution analysis of the time-series by means of Wavelet decomposition and artificial neural networks and achieved around 29% reduction resources without affecting the predictability. Based on wavelet, wavelet packet, time series analysis, and artificial neural networks, Liu et al. [49] developed three hybrid models [Wavelet Packet-BFGS, Wavelet Packet-ARIMA-BFGS and Wavelet-BFGS] and compared the performance with Neuro-Fuzzy, ANFIS (Adaptive Neuro-Fuzzy Inference Systems), Wavelet Packet-RBF (Radial Basis Function) and PM (Persistent Model). The results showed that the proposed hybrid models produced better results than the other models.Most of the above methods use wind speed measurements and predictions at lower heights, while in reality wind energy is generated at hub height. At lower heights, the wind is influenced by ground activities such as heat of the ground, near surface turbulences and human activities. However, at higher heights (more than 80m) these effects are minimized and better predictions are obtained. This paper utilizes machine-learning method to predict wind speeds at different heights and analyzes the predictability of wind speed with height. The paper is organized as follows: Section II discusses the methodology, while Section III is devoted to numerical experimental results. Section IV concludes the paper.

## 2. METHODOLOGY

### 2.1 Recurrent Neural Networks Model

The main purpose of this paper is to analyze correlation of windspeed predictability and its measurement heights. Therefore, a proven WS prediction technique namely the Recurrent Neural Networks (RNN) is utilized to assess the WS predictability with respect to the measurement height. The RNN [50] is one of the NN architectures that represents the information pro–cessing performed by human brain by connecting layers of input and output variables using hidden units. In addition, the RNN also utilizes a feedback from one or more of the hidden units as input to calculate the next output.

Figure 1 shows the architecture of the RNN. The input layer ($X$) is a vector from the past WS values. This paper uses the Elman model where the hidden layer ($H = \{h_0,\ldots h_{N-1}\}$) is computed from a non-linear function of the weighted sum of the input layer and the value of the hidden layer from the previous samples. Mathematically, the output of hidden unit at $k$th sample $h_n(k)$ is given by:

$$h_n(k) = \sigma\left(U_n x(k) + W_h h_n(k-1) + b_n\right) \tag{1}$$

where $U$ denotes the matrix that connects input and hidden layer and $b$ is the bias vector. Matrix W connects the hidden units to the value of units from the previous input sample. The output layer represents the predicted future WS values. The output of $k$th sample $y(k)$ is given by:

$$y(k) = \sigma\left(Vh(k) + b_y\right) \tag{2}$$

where $V$ represents the output layer weights. This paper uses tangent-hyperbolic activation function given by:

$$\sigma(z) = \frac{e^z - e^{-z}}{e^z + e^{-z}} \tag{3}$$

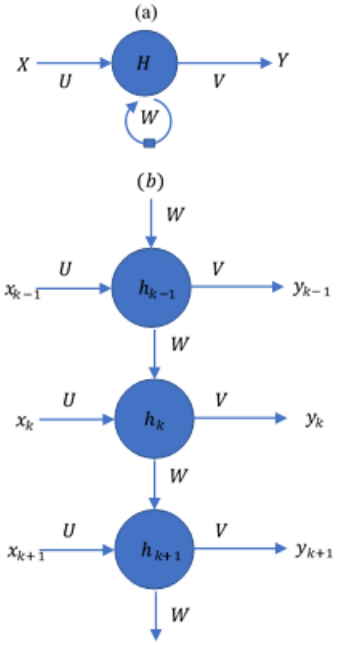


**Figure 1. RNN architecture (a) Recurrent notation (b) Unrolled recurrent architecture**

### 2.2 Levenberg-Marquardt Algorithm for RNN

The Levenberg-Marquardt (LM) algorithm [51]is commonly used to train neural networks due to its speed and guaranteed convergence. Therefore, for neural networks with medium number of units and layers, LM algorithm is the best candidate for the training the RNN. The LM algorithm weights update ($\Delta w$) is given by:

$$\Delta w = -\left[J^T J + \lambda \mathbf{I}\right]^{-1} J^{\mathbf{T}}\left(y - \hat{y}\right) \tag{4}$$

where $J$ denotes the Jacobian matrix of the error function with respect to the weight vector of the RNN. The scalar factor $\lambda$ governs the step size that is decreased if the updates successfully minimize the error function. Otherwise, if the updates failed to reduce the error function, $\lambda$ is increased. The error function is calculated using the difference of the actual values ($y$) and the predicted outputs ($\hat{y}$).

In this paper, three performance measures are employed including mean absolute percent error (MAPE), root mean squared error (RMSE), and the adjusted coefficient of determination ($R^2_{adj}$).These performance measures are calculated using the following equations:

$$MAPE = \frac{1}{N}\sum_{n=1}^{N}\left|\frac{y_n - \hat{y}_n}{y_n}\right| \tag{5}$$

$$RMSE = \sqrt{\frac{\sum_{n=1}^{N}\left(y_n - \hat{y}_n\right)}{N}} \tag{6}$$

$$R^2_{adj} = 1 - \left(1 - R^2\right)\frac{N-1}{N-k} \tag{7}$$

where $N$ denotes the number of samples.Number of inputs is denoted by $k$ and the regular coefficient of determination ($R^2$) is given by

$$R^2 = 1 - \frac{\sum_{n=1}^{N}\left(y_n - \bar{y}\right)^2}{\sum_{n=1}^{N}\left(y_n - \hat{y}\right)^2} \tag{8}$$

where $\bar{y}$ is the mean of the actual data. The regular $R^2$ will always increase when more samples are included while $R^2_{adj}$ corrects for this issue and provides a more solid outcome.

## 3. EXPERIMENTAL RESULTS

This paper utilizes hourly averaged WS data measured by LiDAR system for 90 days between April 2nd and 30th June 2017 where the data was measured at ten different heights namely 20, 40, 50, 60, 80, 100, 120, 140, 160, and 180 m above ground level (AGL). As shown in Figure 2, hourly averaged WS measured at closer to ground level tends to be slower due to friction from the surrounding terrain. The acquired dataset is further divided, where the WS data from the first 80 days is used for training and the remaining for testing.

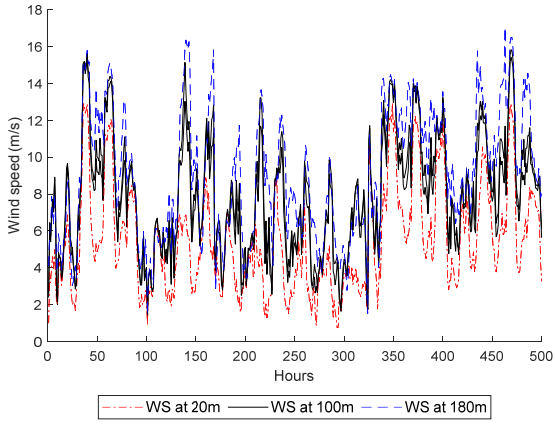


**Figure 2. Measured wind speed at 20m, 100m, and 180m height**

This paper provides WS prediction up to 12 hours ahead of time. For each height, 12 different RNN models were trained as a function of WS values at previous hours to exploit its temporal correlation. Based on the initial experimental results, WS values from 48 previous hours yield more accurate prediction at the future hours. Therefore, all models at each height use the same 48 previous hours WS values as inputs to estimate the WS at the 1st to 12th future hours. Each RNN model uses 48 inputs, 30 hidden units, and a single output. The LM algorithm with scalar factor $\lambda = 3$ and a maximum of 30 iterations exhibited the best performance based on the cross-validation analysis. The training is also terminated when the MSE as the cost function fails to improve more than $10^{-7}$ after six iterations as an indication of convergence. As a comparative method, separate Multilayer-Perceptron (MLP) models were built for predicting WS at the ten heights at 6th hour ahead.

### 3.1 Results and Discussions

The resulting values of the performance parameters such as MAPE, RMSE, and $R^2_{adj}$ are summarized in Tables 1, 2, and 3 respectively for each hour and height. In general, the MAPE values tend to decrease as the prediction height increases (Table 1). For example, the MAPE was 0.15 at 20 m for 1 hour ahead prediction but decreased to 0.11 at 180 m. Similarly, the MAPE values increased with increasing prediction duration as can be observed from column 2 of Table 1. In early hours the MAPE was around 0.15 while for 12-hour duration it increased to 0.19. The RMSE (Table 2) and the adjusted coefficient of determination values (Table 3) do follow the trends of MAPE values presented in Table 1.

The measured and the predicted WS at 20m and 1 hour ahead are compared in Figure 3(a). The predicted WS are found to be in close agreement with the measured values and follow the trend quite closely.

The corresponding scatter plot between the mea–sured and predicted WSs at hour 1, Figure 3(b), shows an adjusted coefficient of determination of 0.91. The predicted and the measured WSs at 12 hours show relatively poor comparison compared to that for 1 hour ahead of time predictions, Figure 3(c), but do follow the trend quite closely. The scatter diagram, Figure 3(d), resulted in $R^2_{adj}$ value of 0.84. At 100m, the comparison between the predicted and the measured WS values at 1 hour (Figure 4(a)) is much better than that at 12 hours (Figure 4(c)). However, in both the cases the predicted WSs follow the trends of measured values closely. The scatter plots for 1 hour (Figure 4(b)) and 12 hours ahead of time predictions show less scatter with $R^2_{adj}$ value of 0.88 at 1 hour compared to that at 12 hours with $R^2_{adj}$ value of 0.77. Similar comparisons are made at 140m and 180m in Figure 5 and 6, respectively. In all of these cases, it is confirmed that the comparisons between the predicted and measured values at hour 1 are much better than those at 12 hours ahead. This observation is further strengthened by the higher values of $R^2_{adj}$ at 1 hour ahead of time predictions than those at 12 hours ahead.

**Table 1. Mean absolute percentage error (MAPE) at different heights and different prediction hours.**

| | 20 m | 40 m | 50 m | 60 m | 80 m | 100 m | 120 m | 140 m | 160 m | 180 m |
|---|---|---|---|---|---|---|---|---|---|---|
| 1 hour | 0.15 | 0.14 | 0.14 | 0.13 | 0.13 | 0.14 | 0.13 | 0.11 | 0.11 | 0.11 |
| 2 hour | 0.16 | 0.14 | 0.14 | 0.13 | 0.14 | 0.14 | 0.13 | 0.14 | 0.12 | 0.12 |
| 3 hour | 0.17 | 0.15 | 0.14 | 0.16 | 0.15 | 0.16 | 0.15 | 0.13 | 0.14 | 0.12 |
| 4 hour | 0.17 | 0.16 | 0.15 | 0.16 | 0.15 | 0.16 | 0.16 | 0.15 | 0.15 | 0.14 |
| 5 hour | 0.18 | 0.16 | 0.15 | 0.17 | 0.17 | 0.17 | 0.14 | 0.15 | 0.16 | 0.14 |
| 6 hour | 0.17 | 0.17 | 0.17 | 0.17 | 0.15 | 0.16 | 0.16 | 0.16 | 0.16 | 0.16 |
| 7 hour | 0.18 | 0.18 | 0.16 | 0.18 | 0.18 | 0.16 | 0.17 | 0.15 | 0.15 | 0.14 |
| 8 hour | 0.18 | 0.18 | 0.17 | 0.18 | 0.18 | 0.18 | 0.18 | 0.18 | 0.17 | 0.15 |
| 9 hour | 0.18 | 0.18 | 0.17 | 0.18 | 0.18 | 0.18 | 0.18 | 0.17 | 0.17 | 0.15 |
| 10 hour | 0.18 | 0.18 | 0.17 | 0.16 | 0.17 | 0.17 | 0.16 | 0.16 | 0.15 | 0.14 |
| 11 hour | 0.19 | 0.19 | 0.17 | 0.17 | 0.16 | 0.16 | 0.16 | 0.16 | 0.16 | 0.16 |
| 12 hour | 0.19 | 0.18 | 0.18 | 0.18 | 0.18 | 0.17 | 0.16 | 0.17 | 0.16 | 0.16 |

**Table 2. Root mean squared error (RMSE) at different heights and different prediction hours.**

| | 20 m | 40 m | 50 m | 60 m | 80 m | 100 m | 120 m | 140 m | 160 m | 180 m |
|---|---|---|---|---|---|---|---|---|---|---|
| 1 hour | 1.06 | 1.05 | 1.03 | 1.01 | 1.00 | 1.00 | 0.99 | 0.97 | 0.95 | 0.95 |
| 2 hour | 1.06 | 1.06 | 1.03 | 1.02 | 1.01 | 1.00 | 1.00 | 0.98 | 0.98 | 0.98 |
| 3 hour | 1.22 | 1.22 | 1.19 | 1.18 | 1.18 | 1.18 | 1.14 | 1.13 | 1.05 | 1.05 |
| 4 hour | 1.18 | 1.26 | 1.24 | 1.24 | 1.23 | 1.21 | 1.21 | 1.19 | 1.19 | 1.17 |
| 5 hour | 1.27 | 1.27 | 1.22 | 1.22 | 1.19 | 1.20 | 1.20 | 1.17 | 1.17 | 1.17 |
| 6 hour | 1.29 | 1.29 | 1.29 | 1.27 | 1.27 | 1.28 | 1.28 | 1.27 | 1.27 | 1.27 |
| 7 hour | 1.42 | 1.41 | 1.42 | 1.40 | 1.40 | 1.40 | 1.33 | 1.30 | 1.28 | 1.26 |
| 8 hour | 1.44 | 1.43 | 1.42 | 1.42 | 1.40 | 1.40 | 1.44 | 1.35 | 1.32 | 1.23 |
| 9 hour | 1.48 | 1.48 | 1.47 | 1.47 | 1.48 | 1.48 | 1.48 | 1.36 | 1.28 | 1.28 |
| 10 hour | 1.51 | 1.50 | 1.48 | 1.48 | 1.47 | 1.48 | 1.47 | 1.36 | 1.31 | 1.31 |
| 11 hour | 1.49 | 1.49 | 1.48 | 1.48 | 1.46 | 1.43 | 1.43 | 1.33 | 1.29 | 1.30 |
| 12 hour | 1.52 | 1.50 | 1.48 | 1.47 | 1.45 | 1.44 | 1.40 | 1.34 | 1.35 | 1.34 |

**Table 3. Adjusted coefficient of determination ($R^2_{adj}$) at different heights and different prediction hours.**

| | 20 m | 40 m | 50 m | 60 m | 80 m | 100 m | 120 m | 140 m | 160 m | 180 m |
|---|---|---|---|---|---|---|---|---|---|---|
| 1 hour | 0.91 | 0.87 | 0.89 | 0.88 | 0.88 | 0.88 | 0.89 | 0.92 | 0.92 | 0.92 |
| 2 hour | 0.87 | 0.87 | 0.85 | 0.85 | 0.87 | 0.87 | 0.88 | 0.88 | 0.92 | 0.92 |
| 3 hour | 0.87 | 0.87 | 0.85 | 0.83 | 0.84 | 0.83 | 0.84 | 0.88 | 0.89 | 0.89 |
| 4 hour | 0.85 | 0.83 | 0.83 | 0.83 | 0.81 | 0.84 | 0.83 | 0.85 | 0.85 | 0.87 |
| 5 hour | 0.85 | 0.83 | 0.84 | 0.80 | 0.83 | 0.81 | 0.85 | 0.87 | 0.87 | 0.87 |
| 6 hour | 0.85 | 0.83 | 0.81 | 0.81 | 0.80 | 0.83 | 0.83 | 0.83 | 0.81 | 0.85 |
| 7 hour | 0.85 | 0.78 | 0.83 | 0.80 | 0.81 | 0.84 | 0.78 | 0.83 | 0.83 | 0.87 |
| 8 hour | 0.85 | 0.80 | 0.80 | 0.77 | 0.76 | 0.80 | 0.78 | 0.81 | 0.82 | 0.87 |
| 9 hour | 0.85 | 0.78 | 0.80 | 0.81 | 0.80 | 0.81 | 0.77 | 0.81 | 0.85 | 0.86 |
| 10 hour | 0.85 | 0.77 | 0.81 | 0.82 | 0.80 | 0.80 | 0.82 | 0.82 | 0.88 | 0.88 |
| 11 hour | 0.84 | 0.80 | 0.80 | 0.78 | 0.78 | 0.82 | 0.81 | 0.82 | 0.85 | 0.86 |
| 12 hour | 0.84 | 0.77 | 0.77 | 0.78 | 0.77 | 0.77 | 0.81 | 0.84 | 0.85 | 0.86 |

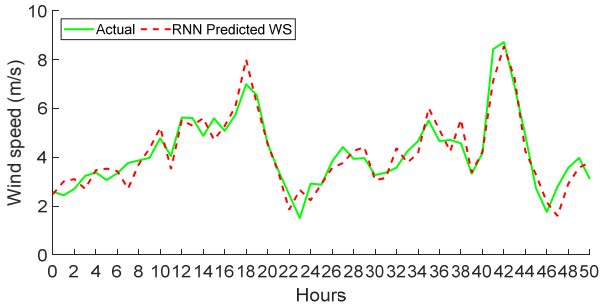


**a) Measured and predicted WS at 20m height and 1 hour ahead**

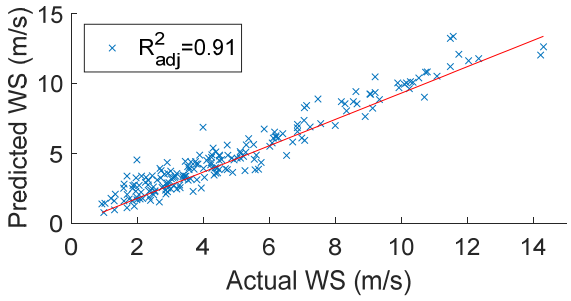


***b)* $R^2_{adj}$ for measured and predicted WS at 20m height and 1 hour ahead**

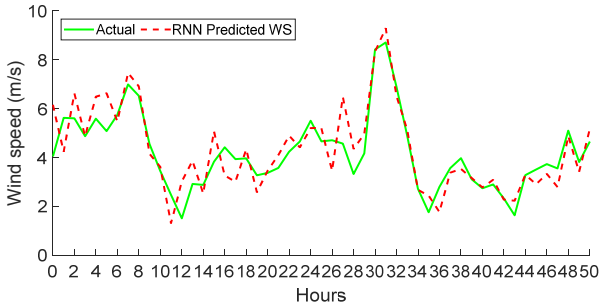


**c) Measured and predicted WS at 20m height and 12 hours ahead**

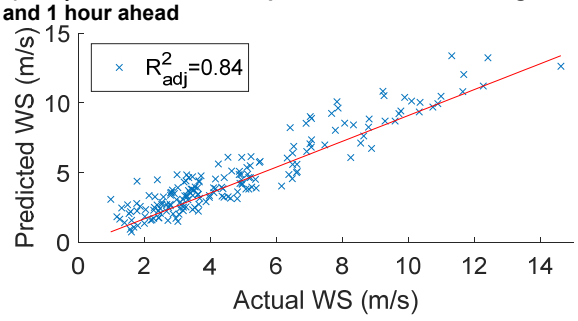


***d)* $R^2_{adj}$ for measured and predicted WS at 20m height and 12 hours ahead**

**Figure 2. Performance at height 10m**

### 3.2 RNN andMLP Models Performance Comparison

In this section, the performance of RNN and MLP methods based on the predictions of WS at 6$^{th}$ future hour and at different heights is compared. The predicted WS values from the two methods are compared with the measurements.

The values of the performance measures RMSE, MAPE, and $R^2_{adj}$ for both the methods are summarized in Table 4. The RMSE are around 1.5 m/s in case of MLP approach and always less than 1.3 m/s in case of RNN method. On the other hand, MAPE values decreased from 0.33 to 0.18 corresponding to 20m and 180 m heights; respectively in case of MLP method while these values decreased to 0.16 at 180m from 0.17 at 20m in case of RNN approach. Relatively smaller magnitudes of RMSE and MAPE along with the higher values of $R^2_{adj}$ are indicative of better perfor–mance of RNN model over MLP approach.

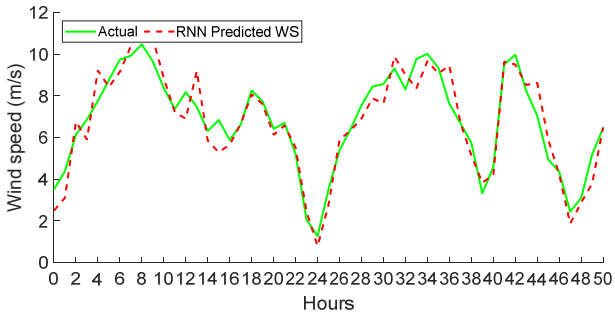


**a) Measured and estimated WS at 100m height and 1 hour ahead**

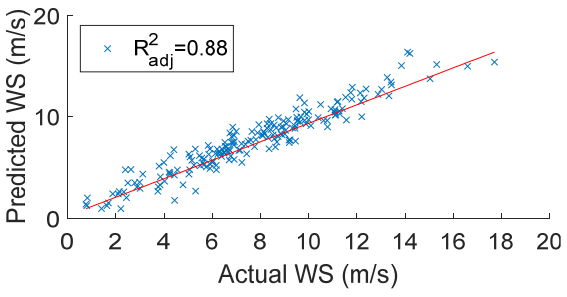


***b)* $R^2_{adj}$ for measured and predicted WS at 100m height and 1 hour ahead**

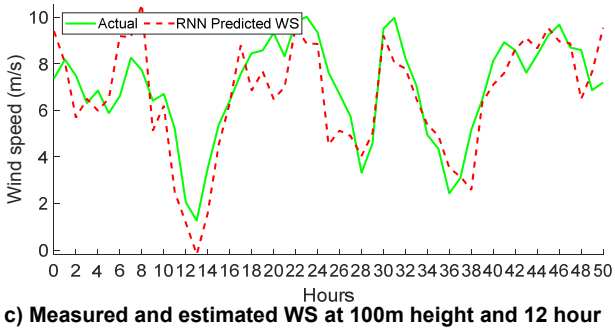


**c) Measured and estimated WS at 100m height and 12 hour ahead**

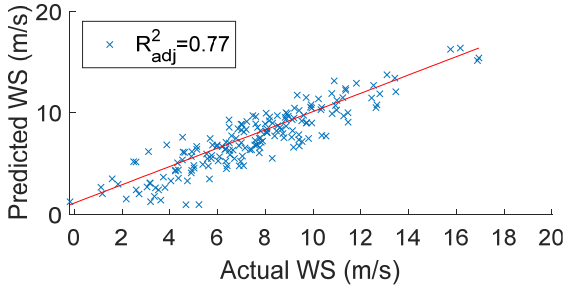


***d)* $R^2_{adj}$ for measured and predicted WS at 100m height and 12 hour ahead**

**Figure 3. Performance at height 100m**

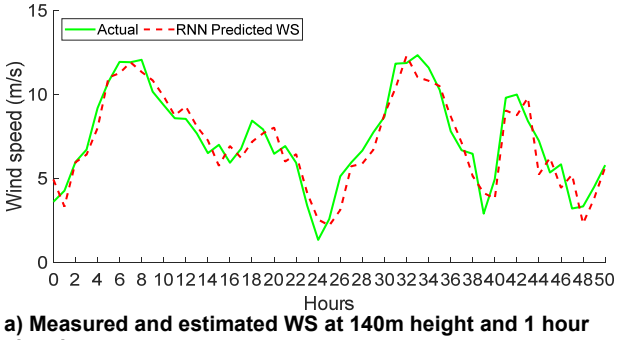


**a) Measured and estimated WS at 140m height and 1 hour ahead**

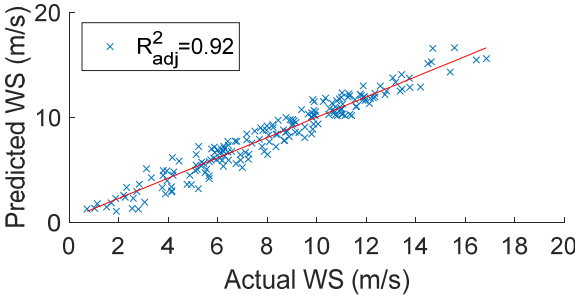


**b) $R^2_{adj}$ for measured and predicted WS at 140m height and 1 hour ahead**

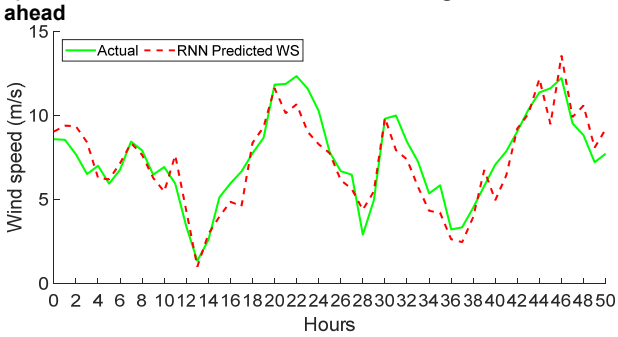


**c) Measured and estimated WS at 140m height and 12 hour ahead**

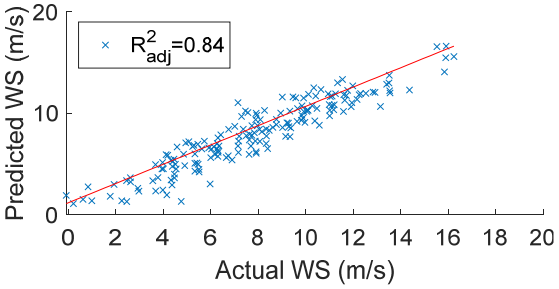


**d) $R^2_{adj}$ for measured and predicted WS at 140m height and 12 hour ahead**

**Figure 4. Performance at height 140m**

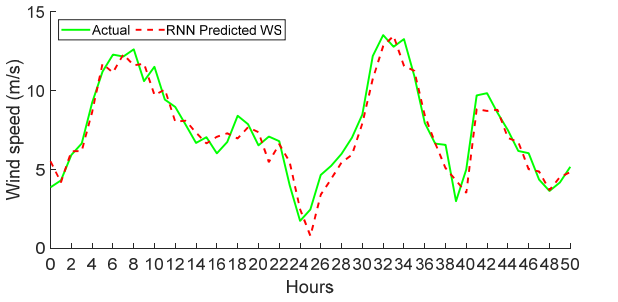


**a) Measured and estimated WS at 180m height and 1 hour ahead**

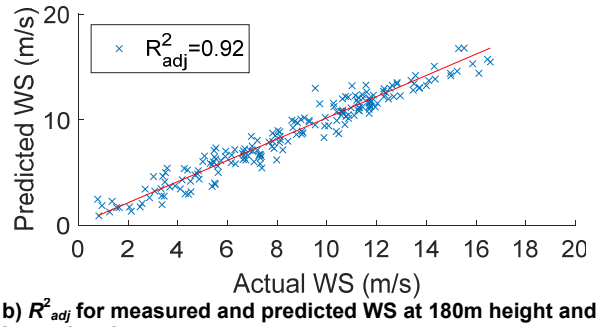


**b) $R^2_{adj}$ for measured and predicted WS at 180m height and 1 hour ahead**

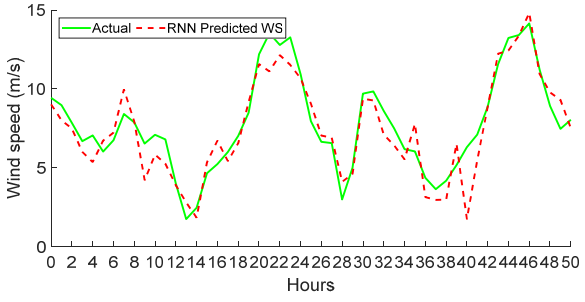


**c) Measured and estimated WS at 180m height and 12 hour ahead**

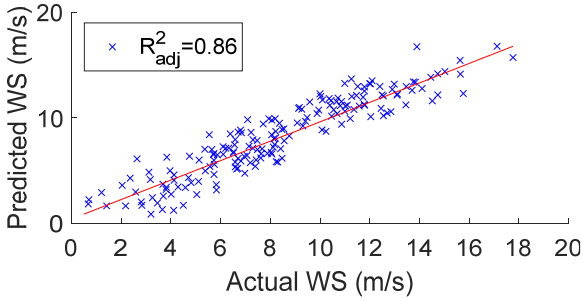


**d) $R^2_{adj}$ for measured and predicted WS at 180m height and 12 hour ahead**

**Figure 5. Performance at height 180m**

The WS values predicted using the two methods are compared with the measured ones at 20, 80, 140, and 180m for the 6th hour and are shown Figure 7. The corresponding scatter plots are also provided in this figure. It is evident from Figure 7(a, c, e, and g) that the comparisons between the predicted and measured WS values keep on improving with increasing height. The corresponding scatter plots shown in Figure 7 (b, d, f, and h) have also confirmed this fact. In these scatter plots, the $R^2_{adj}$ values are found to be larger in the case of RNN methods based prediction compared to those based on MLP methodology. Furthermore, the adjusted coefficient of determination values tends to increase with height, which shows better predictions at higher heights.

**Table 1. Comparison between RNN and MLP model based on estimated wind speed at 6th hour ahead of time.**

| | RMSE | | MAPE | | $R^2_{adj}$ | |
|---|---|---|---|---|---|---|
| | RNN | MLP | RNN | MLP | RNN | MLP |
| 20m | 1.29 | 1.53 | 0.17 | 0.33 | 0.85 | 0.66 |
| 40m | 1.29 | 1.50 | 0.17 | 0.22 | 0.83 | 0.69 |
| 50m | 1.29 | 1.51 | 0.17 | 0.21 | 0.81 | 0.70 |
| 60m | 1.27 | 1.47 | 0.17 | 0.21 | 0.81 | 0.72 |
| 80m | 1.27 | 1.43 | 0.15 | 0.20 | 0.80 | 0.73 |
| 100m | 1.28 | 1.43 | 0.16 | 0.20 | 0.83 | 0.74 |
| 120m | 1.28 | 1.47 | 0.16 | 0.29 | 0.83 | 0.76 |
| 140m | 1.27 | 1.53 | 0.16 | 0.19 | 0.83 | 0.76 |
| 160m | 1.27 | 1.56 | 0.16 | 0.20 | 0.81 | 0.76 |
| 180m | 1.27 | 1.65 | 0.16 | 0.18 | 0.85 | 0.76 |

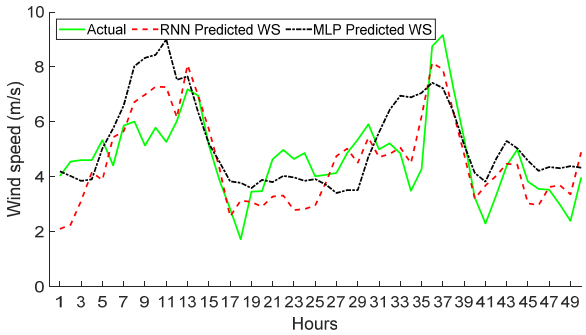


(a) Measured and estimated WS at 20m height

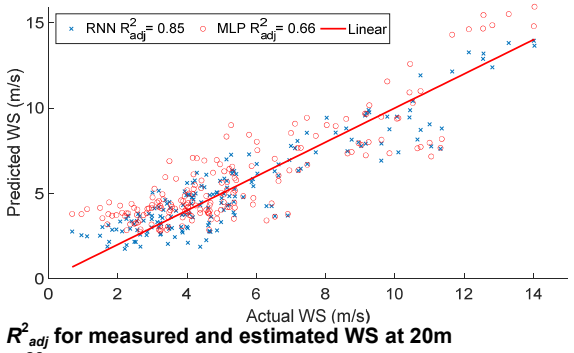


(b) $R^2_{adj}$ for measured and estimated WS at 20m

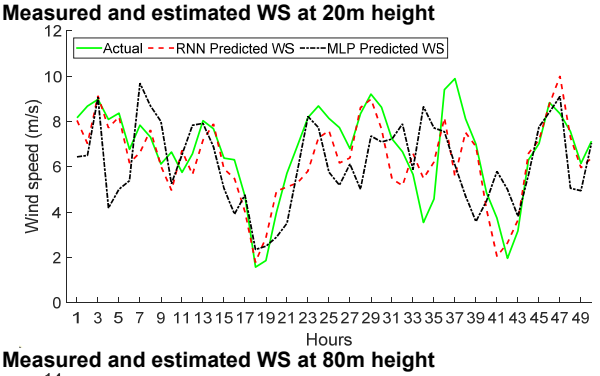


(c) Measured and estimated WS at 80m height

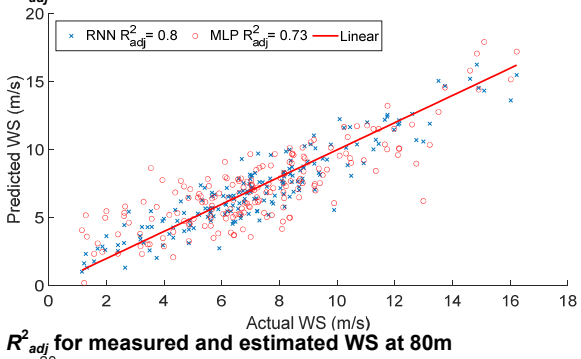


(d) $R^2_{adj}$ for measured and estimated WS at 80m

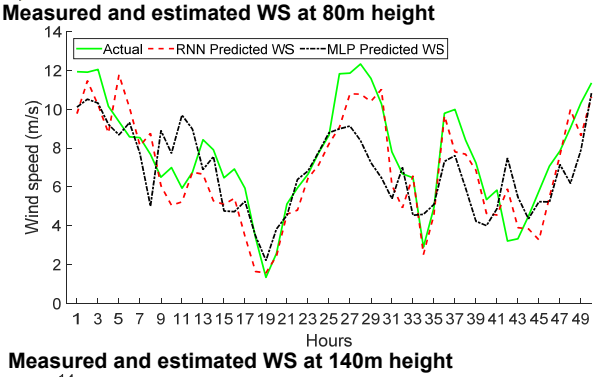


(e) Measured and estimated WS at 140m height

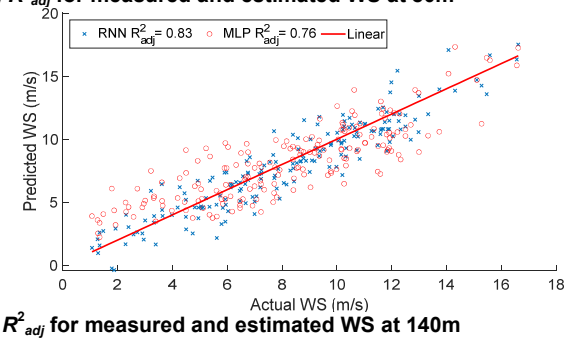


(f) $R^2_{adj}$ for measured and estimated WS at 140m

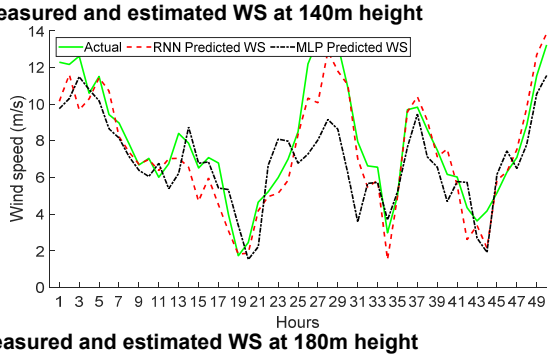


(g) Measured and estimated WS at 180m height

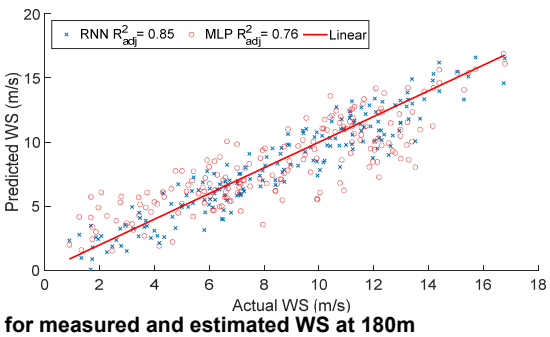


$R^2_{adj}$ for measured and estimated WS at 180m

**Figure 6. Comparison of RNN and MLP at 6th future hour and different heights**

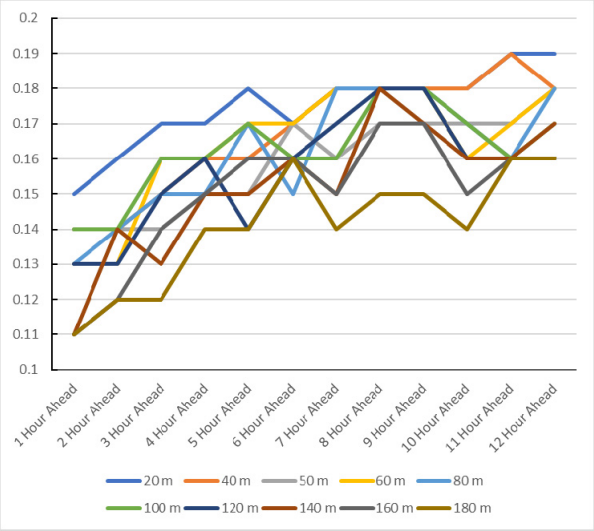


**(a) Variation of MAPE with prediction hour**

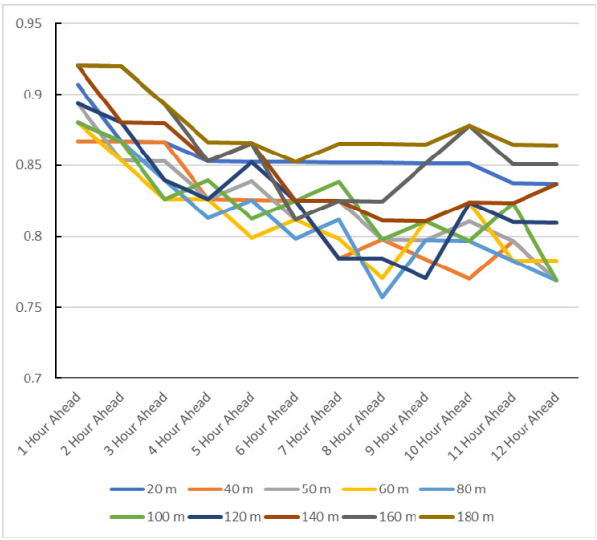


**(b) Variation of $R^2_{adj}$ with prediction hour**

**Figure 7. Predictability in relation to the future hours**

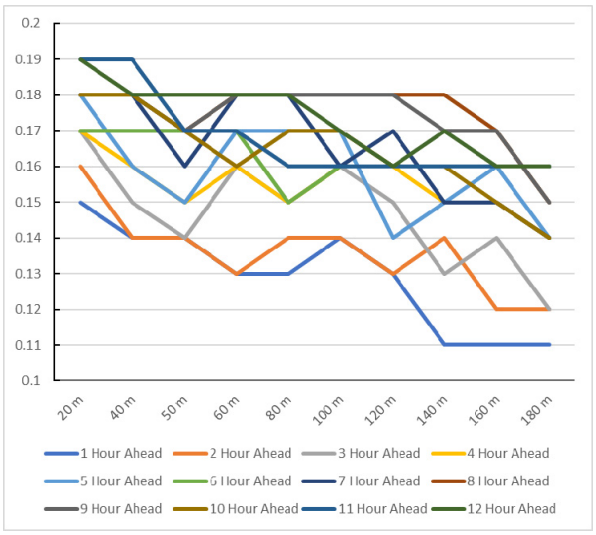


**(a) Variation of MAPE with respect to height**

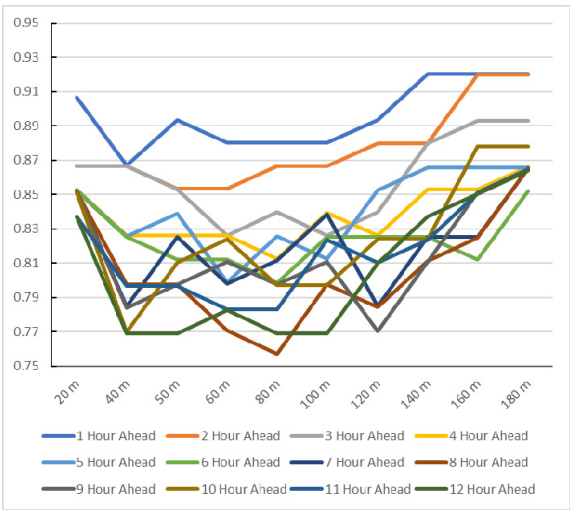


**(b) Variation of $R^2_{adj}$ with respect to height**

**Figure 8. Predictability with heights**

### 3.3 Predictability Analysis of WS with Heights

This sub-section is devoted to the analysis of the predictability of WS with heights. The MAPE and $R^2_{adj}$ values for WS predictions for each of 1 to 12 hours ahead at each height are compared in Figure 8 using RNN. It is seen that as the prediction period in future time domain increases, the MAPE values also increase (Figure 8(a)). In general, a slower increment is observed in the values of MAPE up to hours 6 and a bit faster at further longer time durations. It is also worth mentioning that as the height of prediction increases, the MAPE value decreases. The $R^2_{adj}$ values remained above 0.85 at 180m predictions for all the future hours of prediction (Figure 8(b)). At 20 to 120m heights the $R^2_{adj}$ values between the predicted and the measured WSs are seen to be between 0.8 and 0.9 up to hours 6 and then decreased faster beyond (Figure 8(b)). Figure 9 shows the variation of MAPE and $R^2_{adj}$ with respect to heights using RNN. It can be observed that the performance measures MAPE and $R^2_{adj}$ improve with heights.

## 4. CONCLUSION

An accurate knowledge of future wind speed is critical and also helpful for the estimation of available wind power which is important for utility grid planning and operation. Typically, wind speed measurements are performed at low heights (20-40m). Modern wind turbines operate at hub heights of 80m to 120m. For the first time, to the best of the authorsknowledge, this paper assesses the predictability of wind speed relative to heights. LiDAR device was deployed to collect hourly averaged wind speed data and machine learning method was used for short term prediction of wind speed. Recurrent neural networks (RNN) are used to predict wind speed during next at each of the 12 hours based on previous 48-hour values. Predicted future values from 1st to the 6th hours did not deviate significantly (at height 120m MAPE ranged between 0.13-0.16) compared to the 7th to the 12th future hours (MAPE is increased up to 0.18).

It is observed that the predictability of wind speed improved with increasing heights. The MAPE values decreased from 0.15 at 20m to 0.13 at 120m and further reduced to 0.11 at 180m height for the first hour future wind speed prediction. For the 12th hour future predictions, these values decrease from 0.19 to 0.17, and 0.16 corresponding to heights, 20, 100, 180m, respectively. The coefficient of determination $R^2_{adj}$ for the 12th hour prediction is improved from 0.84 to 0.85 and 0.86 corresponding to heights 20, 160, and 180m, respectively. The proposed method is compared with the multilayer perceptron (MLP)for the prediction of WS at different heights for the 6th future hour. Comparison show that the RNN performed better than MLP in terms of all performance measures.

## ACKNOWLEDGMENT

Authors would like to acknowledge the support of the Deanship of Scientific Research (DSR) at theKing Fahd University of Petroleum & Minerals (KFUPM) provided through project grant DF191024.

## REFERENCES

[1] "Global Wind Report 2021 -Annual market update (GWEC-2021)," 2020.

[2] S. Rehman, M. A. Baseer, and L. M. Alhems, "GIS-based multi-criteria wind farm site selection methodology," *FME Transactions*, vol. 48, no. 4, pp. 855–867, 2020.

[3] R. Carapellucci and L. Giordano, "The effect of diurnal profile and seasonal wind regime on sizing grid-connected and off-grid wind power plants," *Applied Energy*, 2013.

[4] T. P. Chang, "Performance comparison of six numerical methods in estimating Weibull parameters for wind energy application," *Applied Energy*, vol. 88, no. 1, pp. 272–282, 2011.

[5] J. P. S. Catalão, H. M. I. Pousinho, and V. M. F. Mendes, "Short-term wind power forecasting in Portugal by neural networks and wave–let transform," *Renewable Energy*, 2011.

[6] S. A. Akda□, H. S. Bagiorgas, G. Mihalakakou, "Use of two-component Weibull mixtures in the analysis of wind speed in the Eastern Mediterranean," *Applied Energy*, 2010.

[7] H. Aksoy, Z. F. Toprak, A. Aytek, and N. E. Ünal, "Stochastic generation of hourly mean wind speed data," *Renewable Energy*, 2004.

[8] O. A. Jaramillo and M. A. Borja, "Wind speed analysis in La Ventosa , Mexico□: a bimodal probability distribution case," *Renewable Energy*, vol. 29, pp. 1613–1630, 2004.

[9] M. A. Mohandes, S. Rehman, and T. O. Hala–wani, "A neural networks approach for wind speed prediction," *Renewable Energy*, vol. 13, no. 3, pp. 345–354, Mar. 1998.

[10] S. Rehman, N. Natarajan, M. A. Mohandes, and M. M. Alam, "Latitudinal wind power resource assessment along coastal areas of Tamil Nadu, India," *FME Transactions*, vol. 48, no. 3, pp. 566–575, 2020.

[11] N. Natarajan, M. R. Sakthi, S. Rehman, N. S. Shiva, and M. Vasudevan, "Evaluation of Wind Energy Potential of the State of Tamil Nadu, India based on Trend Analysis," *FME Transactions*, vol. 49, no. 1, pp. 244–251, 2020.

[12] B. Rasuo, M. Dinulovic, A. Veg, A. Grbovic, and A. Bengin, "Harmonization of new wind turbine rotor blades development process: A review," *Renewable and Sustainable Energy Reviews*, vol. 39, pp. 874–882, 2014.

[13] T. Kaneko, A. Uehara, T. Senjyu, A. Yona, and N. Urasaki, "An integrated control method for a wind farm to reduce frequency deviations in a small power system," *Applied Energy*. 2011.

[14] B. P. Rasuo and A. C. Bengin, "Optimisation of wind farm layout," *FME Transaction*, vol. 38, no. 3, pp. 107–114, 2010.

[15] B. Rasuo, A. Bengin, A. Veg, "On aerodynamic optimisation of wind farm layout," *Proc. Appl. Math. Mech.*, vol. 10, no. 1, pp. 539–540, 2010.

[16] D. Gupta, V. Kumar, I. Ayus, M. Vasudevan, and N. Natarajan, "Short-Term Prediction of Wind Power Density Using Convolutional LSTM Network," *FME Transaction*, vol. 49, no. 3, pp. 653–663, 2021.

[17] M. Mohandes, T. Halawani, S. Rehman, and A. A. Hussain, "A locally recurrent fuzzy neural network with application to the wind speed prediction using spatial correlation," *Neurocomputing*, vol. 70, no. 79, pp. 1525–1542, 2007.

[18] M. A. Mohandes, T. O. Halawani, S. Rehman, and A. A. Hussain, "Support vector machines for wind speed prediction," *Renewable Energy*, vol. 29, no. 6, 2004.

[19] U. Salman, S. Rehman, B. Alawode, and L. Alhems, "Short Term Prediction of Wind Speed Based on Long-Short Term Memory Networks," *FME Transactions*, vol. 49, pp. 643–652, 2021.

[20] S. Rehman, S. A. Khan, and L. M. Alhems, "The Effect of Acceleration Coefficients in Particle Swarm Optimization Algorithm with Application to Wind Farm Layout Design," *FME Transactions*, 2020.

[21] L. Ye, Y. Zhao, C. Zeng, and C. Zhang, "Short-term wind power prediction based on spatial model," *Renewable Energy*, 2017.

[22] T. Niu, J. Wang, K. Zhang, and P. Du, "Multi-step-ahead wind speed forecasting based on optimal feature selection and a modified bat algorithm with the cognition strategy," *Renewable Energy*, 2018.

[23] S. R. Moreno and L. dos Santos Coelho, "Wind speed forecasting approach based on Singular Spectrum Analysis and Adaptive Neuro Fuzzy Inference System," *Renewable Energy*, 2018.

[24] V. Hoolohan, A. S. Tomlin, and T. Cockerill, "Improved near surface wind speed predictions

using Gaussian process regression combined with numerical weather predictions and obser–ved meteorological data," *Renewable Energy*, 2018.

[25] J. Naik, R. Bisoi, and P. K. Dash, "Prediction interval forecasting of wind speed and wind power using modes decomposition based low rank multi-kernel ridge regression," *Renewable Energy*, 2018.

[26] H. Liu, H. Q. Tian, C. Chen, and Y. fei Li, "A hybrid statistical method to predict wind speed and wind power," *Renewable Energy*, 2010.

[27] H. Liu, C. Chen, H. Q. Tian, and Y. F. Li, "A hybrid model for wind speed prediction using empirical mode decomposition and artificial neural networks," *Renewable Energy*, 2012.

[28] A. Sfetsos, "A comparison of various fore–casting techniques applied to mean hourly wind speed time series," *Renewable Energy*, 2000.

[29] S. A. Kalogirou, S. Panteliou, A. Dentsoras, "Artificial neural networks used for the performance prediction of a thermosiphon solar water heater," *Renewable Energy*, 1999.

[30] A. Şencan, K. A. Yakut, and S. A. Kalogirou, "Thermodynamic analysis of absorption systems using artificial neural network," *Renewable Energy*, vol. 31, no. 1, pp. 29–43, 2006.

[31] A. Mellit and S. A. Kalogirou, "ANFIS-based modelling for photovoltaic power supply system: A case study," *Renewable Energy*, 2011.

[32] A. Mellit, S. A. Kalogirou, and M. Drif, "App–lication of neural networks and genetic algo–rithms for sizing of photovoltaic systems," *Renewable Energy*, 2010.

[33] S. A. Kalogirou, G. A. Florides, P. D. Poulo–upatis, P. Christodoulides, and J. Joseph-Stylianou, "Artificial neural networks for the generation of a conductivity map of the ground," *Renewable Energy*, 2015.

[34] C. Voyant *et al.*, "Machine learning methods for solar radiation forecasting: A review," *Renewable Energy*. 2017.

[35] H. Akçay and T. Filik, "Short-term wind speed forecasting by spectral analysis from long-term observations with missing values," *Applied Energy*, 2017.

[36] Ü. B. Filik and T. Filik, "Wind Speed Prediction Using Artificial Neural Networks Based on Multiple Local Measurements in Eskisehir," in *Energy Procedia*, 2017.

[37] G. Santamaría-Bonfil, A. Reyes-Ballesteros, and C. Gershenson, "Wind speed forecasting for wind farms: A method based on support vector regression," *Renewable Energy*, 2016.

[38] Q. Hu, R. Zhang, Y. Zhou, "Transfer learning for short-term wind speed prediction with deep neural networks," *Renewable Energy*, 2016.

[39] A. Kang, Q. Tan, X. Yuan, X. Lei, and Y. Yuan, "Short-Term Wind Speed Prediction Using EEMD-LSSVM Model," *Advances in Meteorology*, 2017.

[40] H. Liu, H. Q. Tian, X. F. Liang, and Y. F. Li, "Wind speed forecasting approach using secondary decomposition algorithm and Elman neural networks," *Applied Energy*, 2015.

[41] Y. Wang, J. Wang, and X. Wei, "A hybrid wind speed forecasting model based on phase space reconstruction theory and Markov mo–del: A case study of wind farms in northwest China," *Energy*, 2015.

[42] I. Marović, I. Sušanj, and N. Ožanić, "Deve–lopment of ANN model for wind speed prediction as a support for early warning system," *Complexity*, 2017.

[43] O. B. Shukur, M. H. Lee, "Daily wind speed forecasting through hybrid KF-ANN model based on ARIMA," *Renewable Energy*, 2015.

[44] J. Wang, S. Qin, Q. Zhou, and H. Jiang, "Medium-term wind speeds forecasting utilizing hybrid models for three different sites in Xinjiang, China," *Renewable Energy*, 2015.

[45] J. Koo, G. D. Han, H. J. Choi, and J. H. Shim, "Wind-speed prediction and analysis based on geological and distance variables using an artificial neural network: A case study in South Korea," *Energy*, 2015.

[46] X. Wu *et al.*, "A study of single multiplicative neuron model with nonlinear filters for hourly wind speed prediction," *Energy*, 2015.

[47] C. Zhang, H. Wei, J. Zhao, T. Liu, T. Zhu, and K. Zhang, "Short-term wind speed forecasting using empirical mode decomposition and feature selection," *Renewable Energy*, 2016.

[48] B. Doucoure, K. Agbossou, and A. Cardenas, "Time series prediction using artificial wavelet neural network and multi-resolution analysis: Application to wind speed data," *Renewable Energy*, 2016.

[49] H. Liu, H. Q. Tian, D. F. Pan, and Y. F. Li, "Forecasting models for wind speed using wavelet, wavelet packet, time series and Artificial Neural Networks," *Applied Energy*, 2013.

[50] Q. Cao, B. T. Ewing, and M. A. Thompson, "Forecasting wind speed with recurrent neural networks," *European Journal of Operational Research*, 2012.

[51] D. W. Marquardt, "An Algorithm for Least-Squares Estimation of Nonlinear Parameters," *Journal of the Society for Industrial and Applied Mathematics*, 1963.

---

## ТАЧНОСТ ПРЕДВИДЉИВОСТИ БРЗИНЕ ВЕТРА СА ВИСИНОМ КОРИШЋЕЊЕМ РЕКУРЕНТНИХ НЕУРОНСКИХ МРЕЖА

**М. Мохандес, С. Рехман, Х. Нуха, М.С. Ислам, Ф.Х. Шулц**

Тачно предвиђање брзине ветра у будућем вре–менском домену је критично за интегрисање снаге

ветра у мрежу. Брзина ветра се обично мери на мањим висинама док је висина чворишта савремених ветротурбина много већа, 80-120м. Циљ рада је да се оствари боље разумевање предвид–љивости брзине ветра са висином. Подаци о ветру су прикупљени помоћу LiDAR система на висини од 20, 40, 50, 60, 80, 100, 120, 140, 160 и 180 м. Про–сечни подаци по часу су коришћени за обуку и тестирање RNN у циљу предвиђања брзине ветра за сваких будући 12 часова, уз вредности за прет–ходних 48 часова. Детаљна анализа кратко–рочног предвиђања брзине ветра на различитим висинама и будућим часовима показује да се брзина ветра тачније предвиђа на већим висинама. На пример, вредност средње апсолутне процентуалне грешке опада са 0.19 на 0,16 са порастом висине од 20 на 180м, односно за 12. час предвиђања. Перформансе предложеног метода су упоређене са MLP методом. Резултати показују да RNN има боље перформансе него MLP у већем броју случајева приказаних у овом раду у будућем 6. часу.